ACS APPLIED MATERIALS & INTERFACES

Research Article

www.acsami.org

Physically Cross-linked Polymer Binder Induced by Reversible Acid–Base Interaction for High-Performance Silicon Composite Anodes

Sanghyun Lim,[†] Hodong Chu,[†] Kukjoo Lee,[†] Taeeun Yim,[‡] Young-Jun Kim,[‡] Junyoung Mun,*[,§] and Tae-Hyun Kim*[,†]

[†]Organic Material Synthesis Lab, Department of Chemistry, and [§]Department of Energy and Chemical Engineering, Incheon National University, 119 Academy-ro, Songdo-dong, Yeonsu-gu, Incheon 406-772, Korea

[‡]Advanced Batteries Research Center, Korea Electronics Technology Institute, Bundang-gu, Seongnam, Gyeonggi-do 463-816, Korea

Supporting Information

ABSTRACT: Silicon is greatly promising for high-capacity anode materials in lithium-ion batteries (LIBs) due to their exceptionally high theoretical capacity. However, it has a big challenge of severe volume changes during charge and discharge, resulting in substantial deterioration of the electrode and restricting its practical application. This conflict requires a novel binder system enabling reliable cyclability to hold silicon particles without severe disintegration of the electrode. Here, a physically cross-linked polymer binder induced by reversible acid–base interaction is reported for high performance silicon-anodes. Chemical cross-linking of polymer binders, mainly based on acidic polymers including poly(acrylic acid) (PAA), have been suggested as effective ways to accommodate the volume expansion of Si-based electrodes. Unlike the common chemical cross-linking, which causes a gradual and nonreversible fracturing of the cross-linked network, a physically cross-linked binder based on PAA–PBI (poly(benzimidazole)) efficiently holds the Si particles even after the large volume changes due to its ability to reversibly reconstruct ionic bonds. The PBI-containing binder, PAA–PBI-2, exhibited large capacity (1376.7 mAh g^{-1}), high Coulombic efficiency (99.1%) and excellent cyclability (751.0 mAh g^{-1} after 100 cycles). This simple yet efficient method is promising to solve the failures relating with pulverization and isolation from the severe volume changes of the Si electrode, and advance the realization of high-capacity LIBs.

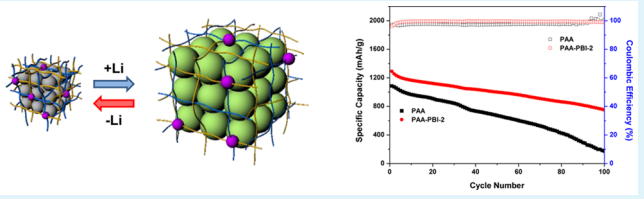

KEYWORDS: *silicon, reversible binder, physically cross-linked binder, poly(acrylic acid), poly(benzimidazole), high capacity anode*

1. INTRODUCTION

The burning of fossil fuels to drive cars, produce electricity, and operate factories has been indicated as a primary cause of global warming. Decreasing the rate at which fossil fuels are burned will require the production of highly energy-efficient equipment such as electric vehicles, but such products rely on systems that can store large amounts of energy, which in turn is continuously increasing the demand for lithium-ion batteries (LIB)s with ever higher energy density.[1,2] Meeting this demand will certainly lead to replacing conventional carbon-based anode materials with the next-generation negative electrode materials that have higher specific energy capacities. Up to now, diverse negative electrode materials, such as hard/soft carbons including graphenes,[3,4] lithium alloys (Si, Sn, Al, Sb, etc.),[5−7] transition-metal oxides (CoO, Co_3O_4, MnO_2, MoO_3, TiO_2, etc.),[8−10] and chalcogenides[11] have been investigated to increase energy density of LIBs. Among them, Si-based anodes in LIBs have been suggested as the most prospective alternatives because of their exceptionally high theoretical capacity (4200 mAh g^{-1}, $Li_{4.4}Si$), low cost, benign effect on the environment, and natural abundance.[6,12−15]

Unlike the conventional graphite anode, utilization of Si as the negative electrode material suffers from substantial volume changes (>400%) during lithiation, which is highly detrimental to the cycle stability of LIB. The mechanical stress caused by this repeated change in volume can fracture the anode composite, hence separating the components of the LIBs from each other, which in turn causes poor electrical contact between the Si particles and severe deterioration of the electrode upon cycling. Even worse, this negative effect becomes more prominent when the electrode is fabricated for the practical high-energy cells, where high mass loading of active materials on the current collector is required.[16]

In general, a Si-based composite anode is built using a composite of Si particles (active material), carbon (conducting agent), and a polymeric binder, and most research efforts have been directed toward the development and modification of various forms of pure silicon,[13] for example, silicon nanotubes,[6] nanoporous silicon,[14] and Si thin platelets,[15] to prevent the deterioration of the reversible capacity of Si-based electrode materials. Despite the improved electrochemical performance of silicon materials, many problems have to be solved to

Received: July 23, 2015
Accepted: October 7, 2015
Published: October 7, 2015

DOI: 10.1021/acsami.5b06682
ACS Appl. Mater. Interfaces 2015, 7, 23545−23553

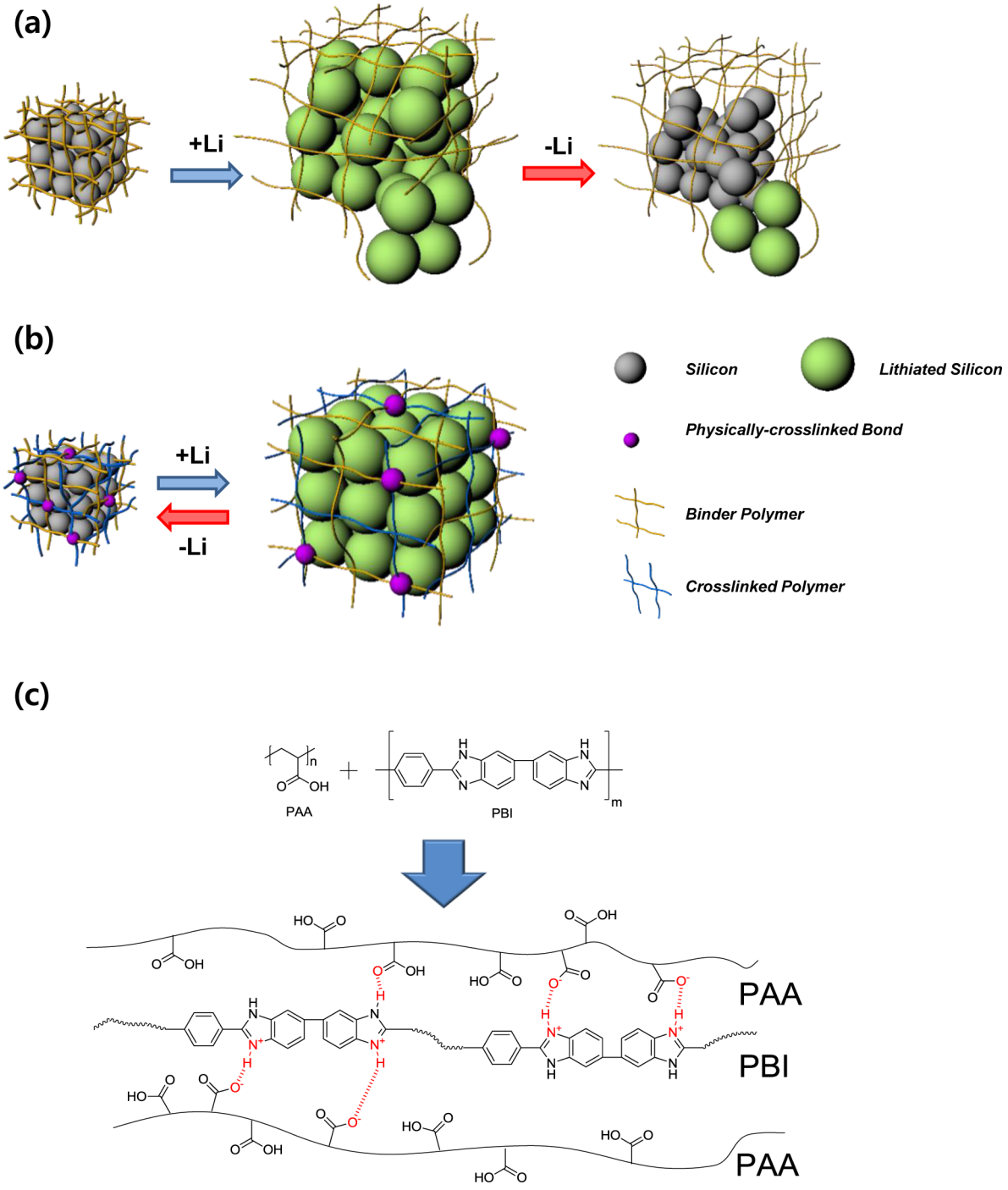

Figure 1. Schematic representation of the technical approaches used to overcome the volume changes of Si particles during cycling. (a) Conventional chemically cross-linked binder whose bonding is irreversible and hence causes fractures in the network upon lithiation (charging) and delithiation (discharging). (b) Physically cross-linked binder that can maintain the interaction between the polymers based on reversible bonding. (c) Molecular interactions of the physically cross-linked polymeric binder through reversible interactions between PAA and PBI.

commercialize them for LIBs, as the large surface areas of Si structures, which result from their small sizes, increase the number of surface failures; these failures lead to poor cyclability, and as a result an excessive amount of supportive inactive components consuming capacity, such as binders and conducting agents, are essential to ensure contacts between particles. Furthermore, the synthesis of nanoarchitectured Si materials requires complicated preparation procedures and hence inevitably increases their production costs.

Recently, many researchers in the battery technology field have been interested in studying polymer binders as simple and cost-effective materials to accommodate the volume expansion of Si-based electrodes.[17−25] Instead of conventional poly(vinylidene fluoride), polymer binders possessing carboxylic groups, such as poly(acrylic acid) (PAA),[26] carboxymethyl cellulose (CMC),[27−29] alginate,[5] and polysaccharide[23] have been proposed to be capable of improving capacity retention of Si-based electrodes. The improvement of the cycle life when using these binders was attributed to the high polymer

DOI: 10.1021/acsami.5b06682
ACS Appl. Mater. Interfaces 2015, 7, 23545−23553

modulus, possibly because of the presence of some extent of self-cross-linked anhydride network formed during the electrode preparation,[30,31] together with the binding between the functional groups (carboxylic acids) of the binder polymers and the partially hydrolyzed surface of the SiO_2 layer of the Si particles. Furthermore, collaborative approaches via alternation of binders expands in the composite materials combining supporting matrix such as carbons and binders.[32]

Chemical cross-linking of alginate,[33] acidic,[30,31,33,34] ionic,[35] and hyperbranch polymeric binders[36] have also been suggested as ways to increase the stability of LIBs with Si-based electrodes. However, even though the three-dimensionally interconnected chemically cross-linked polymers exhibited high mechanical resistance to strain and to nonrecoverable deformation due to the strong interaction between the polymer chains, the nature of chemical cross-linking also increases the stiffness of the polymer network, causing a gradual and nonreversible fracturing of the network,[34−37] and hence leading to eventual decay of the cell performance during long-term battery operation (Figure 1a).

We sought an alternative polymeric binder system that displays reversible formation and deformation of strong molecular interactions between the polymers and that retains its high mechanical strength even after the breakage of the original cross-linking bonds by forming new ones during charge and discharge of Si for LIBs (Figure 1b). Our approach was based on the availability of different types of cross-linking interactions between the macromolecules in polymers, ranging from the very strong covalent bonds that can "fix" the polymer structure and have the greatest impact on the properties of the structure, to physical bonds—such as van der Waals interactions as well as, for many polymers, hydrogen bonding, dipole−dipole, acid−base, and related ionic interactions—which can be dissociated under certain conditions (e.g., elevated temperatures). Although reversible, physical interactions such as hydrogen bonding still impart good levels of chemical and mechanical stability to polymers, with ionic (i.e., electrostatic) interactions being strongest among the physical interactions.

Here we report a novel polymeric binder with electrostatic cross-links induced by a reversible interaction between the acidic PAA and the basic poly(benzimidazole) (PBI) (Figure 1c). PBI is an aromatic macromolecule that possesses both donor and acceptor hydrogen bonding sites that can participate in specific interactions,[38,39] and that produces an imidazolium carboxylate when reacting with PAA (Figure 1c). The PAA−PBI blend binder was shown to endow Si composite electrodes with high mechanical strength of adhesion on Si, and markedly enhanced battery performance compared to those based on just PAA: the designed Si-based composite anode demonstrated an excellent cyclic performance with charge capacity of 751.0 mAh g^{-1} after 100 cycles at a high current density of 1.3 A g^{-1}. Furthermore, unlike other chemically cross-linked binders, which usually involve structural modifications, the synthesis of our new physically cross-linked binder requires simple blending of PAA with PBI, and is therefore very easy to carry out, and is cost-effective as well. To the best of our knowledge, this is the first example of applying physical cross-linking to the development of a polymeric binder to a Si anode with enhanced mechanical properties and resulting improved cell performance.

2. EXPERIMENTAL SECTION

Synthesis of Polybenzimidazole. Polyphosphoric acid (30 g) with a magnetic bar was placed into a round-bottom flask with a N_2 inlet, and was stirred and heated at 100 °C until swirling at moderate viscosity. Then terephthalic acid (0.5 g, 3.01 mmol) and 3,3′-diaminobenzidine (0.645 g, 3.01 mmol) were added slowly. The temperature of the reaction mixture was raised to 200 °C and allowed to stir at this temperature for another 20 h under a nitrogen atmosphere. After this time, the mixture was cooled to room temperature and precipitated into excess water. The solid was collected by filtration and stirred in a 10% K_2CO_3 solution for 24 h. The polymer was again collected by filtration and washed several times with distilled water. Finally, the polymer was dried at 80 °C under vacuum for 24 h to give 0.7 g of the polybenzimidazole as a brown powder. ^{1}H NMR (400 MHz, d_6-DMSO): 13.2−13.4 (br signal, 2H, NH), 8.40 (s, 4H, ArH), 7.4−8.0 (multiplet containing doublet, 6H, J = 8 Hz, ArH); IR (KBr/cm^{-1}) 3432, 3068, 1616, 1398, 1267.

Fabrication of the Si Nanoparticle (SiNP)/Graphite Composite-PAA Electrode. To make a SiNP/graphite composite-PAA electrode, a mixture of the active material (Si nanoparticles (NPs) (Alfa Aesar):graphite (PoscoChemtech) = 3:7), PAA (0.05 g) and conductive carbon (0.05 g, Super P) were dispersed in NMP with a mass ratio of 8:1:1. The PAA−PBI binder solutions were prepared by dissolving PAA (0.69 g) in D.I water (1.28 mL) and PBI (0.014 g for PAA−PBI-2, and 0.036 g for PAA−PBI-5) in DMSO (3 mL) and mixing the two solutions thoroughly before making the PAA−PBI-based electrodes. A mixture of the active material [Si nanoparticles-(NPs-Alfa Aesar): graphite(PoscoChemtech) = 3:7] and conductive carbon (0.704 g for PAA−PBI-2 and 0.726 g for PAA−PBI-5 of Super P) were then dispersed in each binder solution, before the PAA−PBI binder solutions formed precipitation, with a mass ratio of 8:1:1. This slurry was coated onto a Cu foil. As-formed electrodes were dried under vacuum at 120 °C for 1 h. The active materials' loading for all electrodes was fixed at 0.8 mg cm^{-2}.

Characterization and Measurements. ^{1}H NMR spectra were obtained on an Agilent 400-MR (400 MHz) instrument using d_6-DMSO as a reference or internal deuterium lock. FT-IR spectra were recorded on a Varian 640-IR spectrometer. Scanning Electron Microscopy (SEM) was performed using a JEOL JSM-7000F instrument. To see the surface morphology, the cycled Si electrodes were washed with dichloromethane before being imaged. To see the cross-sectional view, specimens were prepared with a JEOL/sn-09010 cross-section polisher.

Peel Test. To determine the adhesion of each binder, we dispersed a mixture of the SiNPs and the binders in NMP with a mass ratio of 3:1. This slurry was then casted onto the Cu foil and dried at 80 °C for 3 h. As-formed electrodes were then further dried under vacuum at 120 °C for another 1 h. The prepared electrodes were cut into 10 mm-wide and 30 mm-long rectangular shapes and attached to 3 M tape. The peel strength of the electrode specimens was recorded with a universal testing machine (UTM, Shimadzu EZ-L). By pulling the tape at a constant displacement rate of 10 mm min^{-1}, the applied force was continuously measured and force-stroke curves were plotted.

Electrochemical Characterization. To evaluate electrochemical performance, we assembled 2032-type coin cells in an Ar-filled glovebox, using porous polyethylene (Celgard 2730) as the separator, lithium discs as the counter electrodes, and 1 M $LiPF_6$ in ethylene carbonate/ethylmethyl carbonate (1:2 v/v) and 10 wt % fluoroethylene carbonate (FEC) (PanaxEtec) were used as electrolytes. In addition, a lithium electrode attached on the long nickel strip was inserted by using an additional separator to prepare 3-electrode cells.[40] The galvanostatic discharge−charge cycling was then performed using a CPS-Lab battery cycler (Basytec) at 25 °C in a temperature-controlled chamber. All the cells were repeatedly discharged to 0.01 V vs Li/Li$^+$ and charged to 1.5 v vs Li/Li$^+$ at a constant C-rate of C/10 in the first 3 cycles for activation and at 1 C in the following cycles. A WBCS-3000 cycler (Wonatech) was used to take GITT measurements. After charging with a current density of 65 mA g^{-1} for an hour, the cell potential was stabilized to OCV for an hour. This was followed

DOI: 10.1021/acsami.5b06682
ACS Appl. Mater. Interfaces 2015, 7, 23545−23553

by the same sequence until the potential fell to 0.01 V vs Li/Li$^+$. The charge capacities were maintained at 1300 mAh g^{-1} by adding a constant-potential step. The discharge sequence was followed by using the same current density until the potential reached 1.5 V.

3. RESULTS AND DISCUSSION

Characterization and Binding Properties. To investigate the interaction between PBI and PAA, we first mixed PAA with two different amounts of PBI (2 wt % relative to PAA (designated as PAA−PBI-2) and 5 wt % relative to PAA (designated as PAA−PBI-5) in NMP without electrode materials. Figure S1 shows a comparison of the FT-IR spectra of PAA and PBI with those of the PAA−PBI blends. Both PAA−PBI-2 and PAA−PBI-5 showed a new characteristic imidazolium carboxylate peak,[39,41] albeit shallow, at around 2550 cm^{-1} due to the formation of an acid−base interaction, and this peak was shifted to lower wavenumbers (2554 cm^{-1} for PAA−PABI-2 and 2545 cm^{-1} for PAA−PBI-5) by increasing the PBI content because of the lowered N−H bond forces caused by increased acid−base (and hence ionic) interactions. These results verify the presence of interactions between the acidic groups in PAA and the basic nitrogens in the PBI cross-linker.

The binding properties of the Si electrode using the PAA−PBI blend binders (PAA−PBI-2 and PAA−PBI-5) were then investigated by first casting the NMP solution of the PAA−PBI blends with the Si electrode on a Cu foil, drying under the conditions used for preparing the composite electrodes, and measuring the strengths of the adhesion to the current collector, i.e., Cu, by applying a 180-degree peel test, which is a widely used method in industry for determining the relative peel resistance of adhesive bonds between adherends and surfaces.[42−44] Peel strength is defined as the force per unit width necessary to initiate failure and maintain a specified rate of failure by means of a stress applied in a peeling mode. Two loads were recorded: (i) static strength (peak load/unit force to initiate peeling); and (ii) average peeling force. These peel strength data were acquired and compared with those of a PAA-based Si electrode (Figure S2 and Table 1).

Table 1. Static Strength and Average Peeling Force for the Si Electrodes with PAA, PAA−PBI-2, and PAA−PBI-5

	static strength (N)	average peeling force (N)
PAA	0.95	0.40
PAA−PBI-2	1.35	0.97
PAA−PBI-5	0.60	0.45

The peel strength data show that the static strength (peak load) of PAA−PBI-2 was higher than those of both PAA and PAA−PBI-5. The relatively high load required to initiate failure of PAA−PBI-2, which as indicated above consists of 2 wt % of PBI, suggests that this binder composition best allocated the carboxylic acid groups of PAA to, on the one hand, formation of hydrogen bonds with hydroxyl groups on the Si, which would directly enhance adhesion to Si, and on the other hand, to the formation of the ionic (imidazolium carboxylate) cross-links with PBI, which also appears to strengthen adhesion to Si,[26,31] apparently indirectly by strengthening the structure of the binder itself. Further increasing amount of the PBI cross-linker to 5 wt % as in PAA−PBI-5, however, apparently weakened adhesion of the binder to Si, probably by tying up too many of the carboxylic acid groups of PAA in the cross-links with PBI and not leaving enough of them free for their essential role in binding to Si.

The average peeling forces of the blend binders (PAA−PBI-2 and PAA−PBI-5) were higher than that of the pristine PAA. Although the peak load described above is closely related to forces of static adhesion, as it measures the force required to initiate peeling, the average peeling force is analogous to the concept behind dynamic friction because the force to maintain a specified rate of failure is measured.[40,43] Therefore, the higher average peeling force value for PAA−PBI blend binders than that of PAA suggests that these binders can, during the dynamic peel test condition, form reversible cross-links, by reforming new acid−base interactions between PAA with the neighboring amine in PBI, even after original cross-links were broken. Note that while the many physically cross-linked sites of the PAA−PBI-5 binder discussed above resulted in a very low peak load (or static strength), lower than the peak load of PAA, they did not prevent the average peeling force from exceeding that of PAA. The PAA, however, having only the chemically cross-linked structure through the anhydride-forming self-condensation reaction between the acid groups, cannot recover cross-linking under the same peel test conditions once the strong covalently cross-linked network is broken, and hence displayed the lowest average peeling force.

Electrochemical Characterization. In this report, we demonstrate the electrochemical performance of composite electrodes containing silicon and graphite as an anode to elucidate the electrochemical performance of the binders.[45] Despite the volume changes of the SiNP/graphite composite electrode would not be around 400% like pure Si electrode, the prepared composite electrodes are considered to exhibit much larger capacity and greater volume changes than the conventional anode electrode like graphite. Hereinafter, we will refer to these types of anodes as the Si electrodes. The first charge/discharge voltage curves of the 2032-type coin half cells with the Si electrode containing different binders are presented in Figure 2a. We also hereinafter refer to lithiation as the charge and delithiation as the discharge, based on the practical applications of the silicon negative electrode. When using LIBs in practice, the first cycle is charged and discharged at a low current to attain the full design capacity and to ensure the capacity balance between the electrodes without kinetic hindrances and polarization effects. To reproduce the sequence of charging and discharging used in practice, we also applied a low current condition of 130 mA g^{-1} (0.1 C) for the first cycle to bypass the kinetic and polarization effects. The overall shapes of all of the initial voltage curves were observed to be similar, indicating that the Si electrodes made of PAA, PAA−PBI-2, and PAA−PBI-5 binders underwent similar electrochemical process. The charge voltage profiles could be mainly divided into two steps: (i) one in which the potential rapidly dropped to 0.1 V vs Li/Li$^+$ and (ii) the other in which the lithiation potential was maintained at this level over a high specific capacity, beyond several hundreds of mAh g^{-1}. The obtained small capacity for which the voltage was greater than 0.1 V was perhaps generated from the formation of solid electrolyte interface related to electrolyte decomposition, and the distinct long plateau under 0.1 V may have originated from the lithiation to the active materials, considering that the capacity under 0.1 V is comparable to the theoretical values (Figure 2a).[46,47]

Especially notable is that the PAA−PBI-2 and PAA−PBI-5 samples yielded no distinct new plateaus in their initial voltage curves compared to that of the PAA sample. These results

DOI: 10.1021/acsami.5b06682
ACS Appl. Mater. Interfaces 2015, 7, 23545−23553

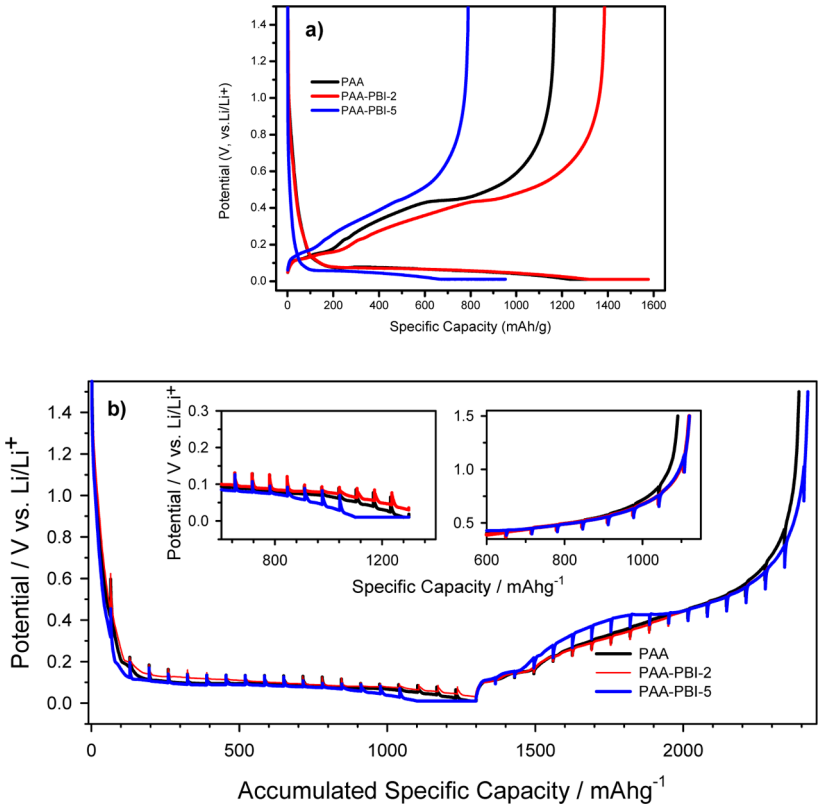

Figure 2. (a) Initial voltage curves of the Si/graphite anode electrodes with the PAA, PAA−PBI-2, and PAA−PBI-5 binders under a charge and discharge current density of 130 mA g^{-1}. (b) Galvanostatic intermittent titration curves of the Si/graphite electrodes with the three different kinds of binders at a charge and discharge current density of 65 mA g^{-1}. Detailed views of the curves at the end of charge (left inset) and discharge (right inset).

indicate little electrochemical decomposition of other components at the first voltage curves, and confirm that our new PBI-containing binders did not electrochemically broken down and were stable at least in the potential range of the Si electrode from 1.5 to 0 V vs Li/Li^+. Such stability, in particular the avoidance of unfavorable electrochemical decompositions in the potential range of LIBs, is a prerequisite for the binder to serve as a component of LIBs.

Despite the low current density applied at the first cycle, the specific capacities of the samples (at 1577 mA g^{-1} for PAA−PBI-2, 1416 mA g^{-1} for PAA, and 952 mA g^{-1} for PAA−PBI-5 (Figure 2a)) differed considerably. The relatively high lithiation capacity for PAA−PBI-2 is ascribed to the enhanced mechanical strength of this binder which can accommodate the physical stress incurred during the volume expansion of the Si electrode. In contrast, the cell with PAA−PBI-5 binder, which was shown to have the weakest static adhesion, showed the lowest capacity even at the first charge. It is believed that weak binding force caused by the PAA−PBI-5 decreases electron pathway because of losing the connectivity among the active material, supporting carbon agent and the current collector in the Si composite electrode. Such different binding forces can lead different kinetic hindrances. Overall, the charge capacities of the cells more or less reflected the mechanical strengths of the binders (Table 1).

At the subsequent discharge, the voltage curves of all three samples showed plateaus corresponding to delithiation from the active materials, and the electrode with PAA−PBI-2, in particular, displayed superior reversible discharge capacity compared to the electrodes with PAA and PAA−PBI-5. Typically, a large part of the irreversible capacity originates from the isolated lithiated Si particles because the silicon electrode inevitably undergoes a large volume expansion and shrinkage during the lithiation/delithiation process: during the lithiation of Si (charge), the large volume expansion of the Si active material causes the chemical bonds of typical binders such as PAA to rupture, hence reducing the adhesive forces of such binders; at the subsequent discharge, the volume contraction combined with the degeneration of the binders may result in the electrode components falling apart. Although binders like PAA that rely on chemical (i.e., covalent) linkages cannot reform such bonds after any original ones were broken during discharge, the integrity of our new PBI-containing binders were designed to rely on physical bonds so that new ionic interactions between carboxylate group in PAA and imidazolium in PBI (through hydrogen bonds between acidic PAA and basic PBI) can be formed even after the original chemical bonds were broken by Si volume changes during cycling. Such a mechanism would be expected to relieve fading of a PBI-containing binder, and hence help prevent unfavorable resistance after the charging and discharging process that would result from such fading. The Coulombic efficiencies of the first cycles of the electrodes containing PAA−PBI-2, PAA, and PAA−PBI-5 were determined to be 87.3, 82.4, and 82.9%, respectively, by calculating the ratio of the first discharge and charge capacity, and the relatively high value for PAA−PBI-2 supports our hypothesis that hydrogen-bonded cross-links between PAA and PBI can form after initial ruptures.

Although the Coulombic efficiency of the cell with PAA−PBI-5 was a little higher than that of the cell with PAA, it was

DOI: 10.1021/acsami.5b06682
ACS Appl. Mater. Interfaces 2015, 7, 23545−23553

difficult to conclude that the PBI in this case also had a role in reforming cross-links due to their uncontrolled specific charge capacities leading to an unexpected effect such as unequable physical stress, volume change, Si isolation, and electrolyte decomposition caused by different depth of charge. To overcome these obstacles resulting from the different charge capacities and trace the electrochemical behavior in detail, we applied the galvanostatic intermittent titration technique (GITT): especially the specific charge capacity was controlled to 1300 mAh g^{-1} by applying a very low current density of 65 mA g^{-1} (0.05 *C*) and subsequent constant potential step of 0.01 V (Figure 2b). As shown in the left inset of Figure 2b, the cell with PAA−PBI-5 exhibited the greatest polarization because the potential dropped to below the cutoff potential of 0.1 V vs Li/Li^+ at the lowest charge potential among the electrode samples. Meanwhile, the polarization of the cell with PAA−PBI-2 was the lowest. These behaviors are considered to have originated from the different static strength characteristics of the binders, as was described above in Figure 2a.

Similarly, at the early stage of the following discharge in the range of the accumulated specific capacity from 1450 to 1950 mAh g^{-1}, the polarization of the Si electrode with PAA−PBI-5 was highest among the three cells, showing the same behavior of high kinetic hindrance as the results obtained from the initial voltage curves and the static strength characteristics. The evidence for reversible bonding for the PAA−PBI-5 binder, however, was observed at the end of the discharge: on discharging, the polarization of the Si electrode with PAA binder suddenly increased to beyond 900 mAh g^{-1} with a low Coulombic efficiency of 83.9%, as depicted in the right inset of Figure 2b, whereas both cells with PBI-containing binders (i.e., PAA−PBI-2 and PAA−PBI-5) displayed the same specific discharge capacities. Perhaps the reduction of volume as the delithiation proceeded and resulting detachment of the PAA binder caused the sudden polarization for this cell at the end of discharge, but this issue was mitigated for the cells with the PBI-containing binders because of reversible bonding.

Furthermore, the cell with PAA−PBI-5, unlike the case measured at the constant current charge and discharge shown in Figure 2a, showed a high Coulombic efficiency of 86.2%, as high as the cell with PAA−PBI-2, and this result is again ascribed to the reversible bonding characteristics that relieve the effects of poor kinetic hindrance applied at low current. These results all show that the PBI-containing binders (PAA−PBI-2 and PAA−PBI-5) can function as reversible binders, holding the active materials together during the severe shrinkage. Meanwhile, the decreased Coulombic efficiency of PAA−PBI-2 in the GITT experiment (Figure 2b) compared to the Coulombic efficiency of PAA−PBI-2 derived from the galvanostatic chage/discharge experiment (Figure 2a) may have originated from the restricted lithiation depth at the maintained specific charge capacity of 1300 mAh g^{-1}. Because high Coulombic efficiency is one of the most important factors for an LIB, with its restricted electrode mass and volume, to attain a large capacity, the high initial Coulombic efficiency for the electrodes containing PBI are expected to lead to the development of large-capacity LIBs, which will be useful for EVs and ESS systems. Despite its reversible bonding, the PAA−PBI-5 was regarded as unsuitable as a binder, given the fact that the electrode with this binder exhibited very low initial capacity, probably caused by its very poor mechanical properties (static adhesion). We do, however, conclude that the PBI-containing binders (PAA−PBI-2 and PAA−PBI-5) can at least improve the Coulombic efficiency of the first cycle by virtue of their reversible physical bonding.

After the initial cycle, the available discharge capacity of the electrode with PAA−PBI-2 (1292 mAh g^{-1}) was also higher than the corresponding capacities of the PAA and PAA−PBI-5 electrodes (1087 and 730 mAh g^{-1}, respectively) (Figure 3).

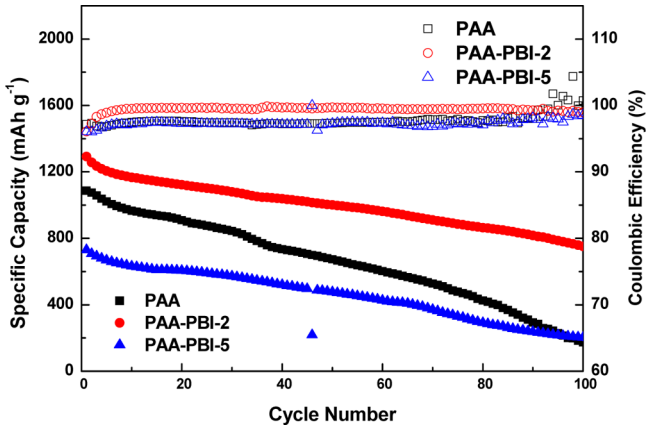

Figure 3. Cycling performance (filled dots) and the Coulombic efficiency (vacant dots) from the 2032 type coin cells containing Si/graphite anode electrodes with the PAA, PAA−PBI-2, and PAA−PBI-5 binders (potential range, 0.01−1.5; current density, 130 mA g^{-1} and 25 °C).

Furthermore, our new PAA−PBI-2 binder effectively improved the cyclability for the subsequent cycles. It is noteworthy to mention that the cyclability of the electrode with the PAA−PBI-2 binder, if only the active materials were considered, was expected to be lower because of large volume changes resulting from its high capacities, but the cyclability of PAA−PBI-2 was indeed much higher than that of the reference sample (PAA). The high mechanical strength (static adhesion property) and reversible physical bonding of this PAA−PBI-2 binder are believed to have yielded the high capacity of its cell for many cycles.

The electrochemical internal resistance behavior of the electrodes with two different binders (PAA and PAA−PBI-2) was further evaluated by the AC impedance method upon cycling. The results obtained from the fully discharged 3-electrode coin type cell after the first, 10th and 50th cycles are shown in Figure S3. The Nyquist plots measured from each cell displayed two semicircles that could be fitted by the proposed equivalent circuit in the inset of Figure S3a. The diameters of the semicircles at the high frequency and low frequency can be respectively assigned to the resistance of the surface and the resistance of the charge transfer during the electrochemical reactions. For both samples, all resistances of the cell increased with continued cycling due to deterioration of the binder caused by the repeated volume changes of Si electrode, suggesting that an increased resistance of the cell caused by binder deterioration may influence the cyclability of the cells. The resistance increased relatively slowly, however, for the cell of the electrode containing the PAA−PBI-2 binder. In general cases, large changes in the volume of Si electrodes and poor mechanical strength of binders can cause loose electrical contacts between particles, the PAA−PBI-2 binder, because of its reversible bond-forming nature and good adhesion, contributed to the reduced internal resistance in the impedance analysis of its cell.

DOI: 10.1021/acsami.5b06682
ACS Appl. Mater. Interfaces 2015, 7, 23545−23553

As expected, the average Coulombic efficiency over 100 cycles of the electrode with PAA−PBI-2 was, at 99.1%, highest among the three binders (PAA, PAA−PBI-2, and PAA−PBI-5) studied (unfilled dots in Figure 3). The volume reduction during the charging at the initial cycle as well as the subsequent cycles generally drives irreversible capacity by pulverization and formation of cracks in the electrode, and eventually leads to poor Coulombic efficiency. The high Coulombic efficiency for the electrode with PAA−PBI-2 binder is, therefore, related to the high mechanical strength, together with reversible physical bonding property, of this binder, and is also in accordance with the relatively good cyclability for this binder.

Morphology Characterization. The electrode morphology was imaged using FE-SEM, and top and cross-sectional views were obtained. These images are highly consistent with the results of the mechanical and electrochemical analyses. The electrodes containing PAA and PAA−PBI-2 both showed homogeneous surfaces prior to cycling (Figure 4a and b), and cracks after cycling (Figure 4c and 4d), as would be expected from large volume changes during charge and discharge. Moreover, although the volume change of the electrode with PAA−PBI-2 was as mentioned above expected to be higher than that of the PAA-based electrode, the electrode containing PAA−PBI-2 nevertheless revealed fewer and narrower cracks in the FE-SEM images compared to the electrode with PAA. This result, like the other results above, appears to be due to the high mechanical strength and reversible cross-linking of the PAA−PBI-2 binder, which apparently held the Si particles tightly, causing fewer fissures in its electrode.

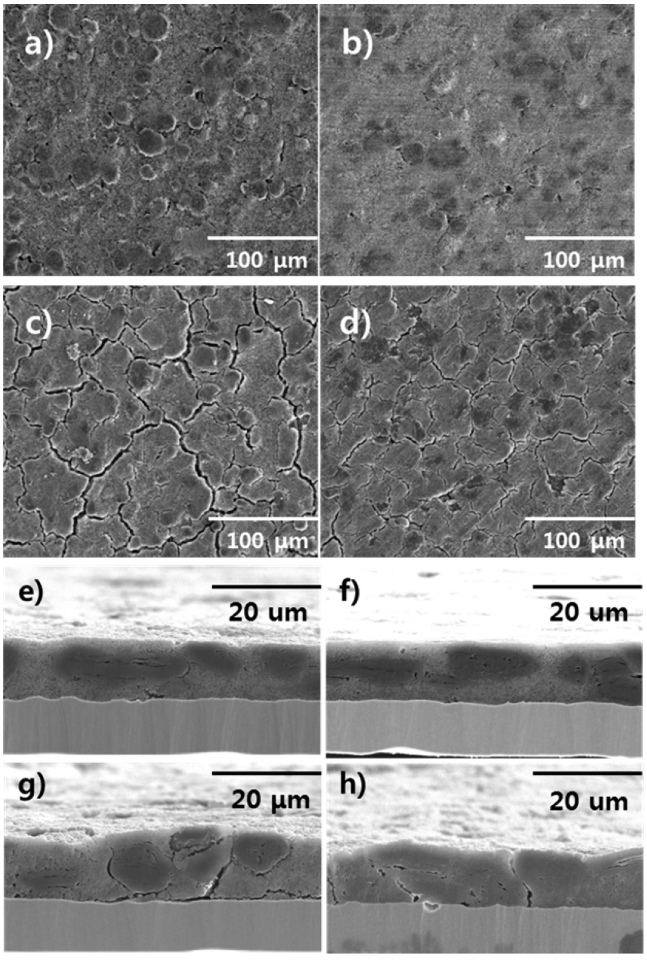

Figure 4. FE-SEM images of the Si/graphite electrodes. (a) Pristine electrode with the PAA binder and (b) that with the PAA−PBI-2 binder. (c) Electrode with the PAA binder after one cycle and (d) that with the PAA−PBI-2 binder after one cycle. (e−h) Cross-sectional FE-SEM images by using FIB treatments: (e) pristine electrode with PAA, (f) pristine electrode with PAA−PBI-2, (g) electrode with PAA after one cycle, and (h) that with PAA−PBI-2 after one cycle.

The swelling of these two electrodes (i.e., containing PAA and PAA−PBI-2) after the discharge was also examined (Figure 4e, f). Initially, the thickness of each electrode was controlled to be the same, at about 11 um, to eliminate the effect of the loading level (Figure 4e, f). Interestingly, the thickness of the electrode with the PAA−PBI-2 binder almost recovered its original value even after cycling the cell once (Figure 4h), whereas the electrode with PAA instead displayed a volume expansion of ca. 14% (Figure 4g).

In addition to the expanded volume of the PAA-containing electrode, and its many cracks as seen in the cross-sectional as well as top-view images, delamination of this electrode from the current collector was also observed, which may have caused the high resistance and polarization of this electrode. In contrast, a highly improved and reversible morphology resulted for the electrode with the PAA−PBI-2 binder, which is in accordance with its high Coulombic efficiency in the cycling test.

4. CONCLUSIONS

In summary, we have demonstrated that a physically cross-linked binder containing PBI as a component efficiently held onto the Si particles even after the large volume changes because of its ability to reversibly reconstruct ionic bonds. The PBI-containing binders tested, PAA−PBI-2 and PAA−PBI-5, exhibited improved static strength and reversible forces in the mechanical analyses. The PAA−PBI-2 binder also concomitantly yielded a Si electrode with large capacity (1376.7 mAh g^{-1}), high Coulombic efficiency (initial: 87.3 and average: 99.1%) and excellent cyclability (751.0 mAh g^{-1} after 100 cycles). It is expected that such physically cross-linked polymeric binders could solve the failures relating with pulverization and isolation from the severe volume changes of the Si electrode, and advance the realization of high-capacity LIBs for large power sources of EVs and ESS systems.

■ ASSOCIATED CONTENT

Supporting Information

The Supporting Information is available free of charge on the ACS Publications website at DOI: 10.1021/acsami.5b06682.

Detailed experimental procedures, characterizations, and further electrochemical properties (PDF)

■ AUTHOR INFORMATION

Corresponding Authors

*E-mail: jymun@inu.ac.kr.
*E-mail: tkim@inu.ac.kr.

Notes

The authors declare no competing financial interest.

■ ACKNOWLEDGMENTS

This work was supported by the IT R&D program of MKE/KEIT(10044962).

DOI: 10.1021/acsami.5b06682
ACS Appl. Mater. Interfaces 2015, 7, 23545−23553

REFERENCES

(1) Armand, M.; Tarascon, J.-M. Building Better Batteries. *Nature* **2008**, *451*, 652−657.

(2) Yu, M.; Wang, A.; Wang, Y.; Li, C.; Shi, G. An Alumina Stabilized ZnO−graphene Anode for Lithium Ion Batteries via Atomic Layer Deposition. *Nanoscale* **2014**, *6*, 11419−11424.

(3) Lee, K. T.; Lytle, J. C.; Ergang, N. S.; Stein, A. Synthesis and Rate Performance of Monolithic Macroporous Carbon Electrodes for Lithium-ion Secondary Batteries. *Adv. Funct. Mater.* **2005**, *15*, 547−556.

(4) Zhou, G.; Li, F.; Cheng, H.-M. Progress in Flexible Lithium Batteries and Future Prospects. *Energy Environ. Sci.* **2014**, *7*, 1307−1338.

(5) Kovalenko, I.; Zdyrko, B.; Magasinski, A.; Hertzberg, B.; Milicev, Z.; Burtovyy, R.; Luzinov, I.; Yushin, G. A Major Constituent of Brown Algae for Use in High-capacity Li-ion Batteries. *Science* **2011**, *334*, 75−79.

(6) Wu, H.; Chan, G.; Choi, J. W.; Yao, Y.; McDowell, M. T.; Lee, S. W.; Jackson, A.; Yang, Y.; Hu, L.; Cui, Y. Stable Cycling of Double-walled Silicon Nanotube Battery Anodes through Solid-electrolyte Interphase Control. *Nat. Nanotechnol.* **2012**, *7*, 310−315.

(7) Park, S.; Ryu, J. H.; Oh, S. M. Passivating Ability of Surface Film Derived from Vinylene Carbonate on Tin Negative Electrode. *J. Electrochem. Soc.* **2011**, *158*, A498−A503.

(8) Wang, X.; Yan, Y.; Hao, B.; Chen, G. Protein-Mediated Layer-by-Layer Synthesis of TiO_2 (B)/Anatase/Carbon Coating on Nickel Foam as Negative Electrode Material for Lithium-Ion Battery. *ACS Appl. Mater. Interfaces* **2013**, *5*, 3631−3637.

(9) Xiao, X.; Liu, X.; Zhao, H.; Chen, D.; Liu, F.; Xiang, J.; Hu, Z.; Li, Y. Facile Shape Control of Co3O4 and the Effect of the Crystal Plane on Electrochemical Performance. *Adv. Mater.* **2012**, *24*, 5762−5766.

(10) Yu, M.; Yuan, W.; Li, C.; Hong, J.-D.; Shi, G. Performance Enhancement of a Graphene−Sulfur Composite as a Lithium−sulfur Battery Electrode by Coating with an Ultrathin Al_2O_3 Film via Atomic Layer Deposition. *J. Mater. Chem. A* **2014**, *2*, 7360−7366.

(11) Yu, M.; Zhu, C.; Zhang, K.; Chen, Y.; Li, C.; Gao, P.; Yang, P.; Ouyang, Q. Three-dimensional Hierarchical MoS_2 Nanoflake Array/carbon Cloth as High-performance Flexible Lithium-ion Battery Anodes. *J. Mater. Chem. A* **2014**, *2*, 4551−4557.

(12) Obrovac, M.; Christensen, L. Structural Changes in Silicon Anodes during Lithium Insertion/extraction. *Electrochem. Solid-State Lett.* **2004**, *7*, A93−A96.

(13) Szczech, J. R.; Jin, S. Nanostructured Silicon for High Capacity Lithium Battery Anodes. *Energy Environ. Sci.* **2011**, *4*, 56−72.

(14) Lee, J. I.; Lee, K. T.; Cho, J.; Kim, J.; Choi, N. S.; Park, S. Chemical-Assisted Thermal Disproportionation of Porous Silicon Monoxide into Silicon-Based Multicomponent Systems. *Angew. Chem., Int. Ed.* **2012**, *51*, 2767−2771.

(15) Saito, M.; Nakai, K.; Yamada, T.; Takenaka, T.; Hirota, M.; Kamei, A.; Tasaka, A.; Inaba, M. Si Thin Platelets as High-capacity Negative Electrode for Li-ion Batteries. *J. Power Sources* **2011**, *196*, 6637−6643.

(16) Liu, N.; Lu, Z.; Zhao, J.; McDowell, M. T.; Lee, H.-W.; Zhao, W.; Cui, Y. A Pomegranate-inspired Nanoscale Design for Large-volume-change Lithium Battery Anodes. *Nat. Nanotechnol.* **2014**, *9*, 187−192.

(17) Cui, L.-F.; Hu, L.; Wu, H.; Choi, J. W.; Cui, Y. Inorganic Glue Enabling High Performance of Silicon Particles as Lithium Ion Battery Anode. *J. Electrochem. Soc.* **2011**, *158*, A592−A596.

(18) Choi, N.-S.; Yew, K. H.; Choi, W.-U.; Kim, S.-S. Enhanced Electrochemical Properties of a Si-based Anode Using an Electrochemically Active Polyamide Imide Binder. *J. Power Sources* **2008**, *177*, 590−594.

(19) Garsuch, R. R.; Le, D.-B.; Garsuch, A.; Li, J.; Wang, S.; Farooq, A.; Dahn, J. Studies of Lithium-exchanged Nafion as an Electrode Binder for Alloy Negatives in Lithium-ion batteries. *J. Electrochem. Soc.* **2008**, *155*, A721−A724.

(20) Liu, G.; Xun, S.; Vukmirovic, N.; Song, X.; Olalde-Velasco, P.; Zheng, H.; Battaglia, V. S.; Wang, L.; Yang, W. Polymers with Tailored Electronic Structure for High Capacity Lithium Battery Electrodes. *Adv. Mater.* **2011**, *23*, 4679−4683.

(21) Hochgatterer, N.; Schweiger, M.; Koller, S.; Raimann, P.; Wöhrle, T.; Wurm, C.; Winter, M. Silicon/graphite Composite Electrodes for High-capacity Anodes: Influence of Binder Chemistry on Cycling Stability. *Electrochem. Solid-State Lett.* **2008**, *11*, A76−A80.

(22) Ryou, M. H.; Kim, J.; Lee, I.; Kim, S.; Jeong, Y. K.; Hong, S.; Ryu, J. H.; Kim, T. S.; Park, J. K.; Lee, H.; Choi, J. W. Mussel-inspired Adhesive Binders for High-performance Silicon Nanoparticle Anodes in Lithium-ion Batteries. *Adv. Mater.* **2013**, *25*, 1571−1576.

(23) Jeong, Y. K.; Kwon, T.-w.; Lee, I.; Kim, T.-S.; Coskun, A.; Choi, J. W. Millipede-inspired Structural Design Principle for High Performance Polysaccharide Binders in Silicon Anodes. *Energy Environ. Sci.* **2015**, *8*, 1224−1230.

(24) Chen, Z.; Wang, C.; Lopez, J.; Lu, Z.; Cui, Y.; Bao, Z., High-Areal-Capacity Silicon Electrodes with Low-Cost Silicon Particles Based on Spatial Control of Self-Healing Binder. *Adv. Energy Mater.* **2015**, *5*, 10.1002/aenm.201401826.

(25) Jeena, M.; Lee, J.-I.; Kim, S. H.; Kim, C.; Kim, J.-Y.; Park, S.; Ryu, J.-H. Multifunctional Molecular Design as an Efficient Polymeric Binder for Silicon Anodes in Lithium-Ion Batteries. *ACS Appl. Mater. Interfaces* **2014**, *6*, 18001−18007.

(26) Magasinski, A.; Zdyrko, B.; Kovalenko, I.; Hertzberg, B.; Burtovyy, R.; Huebner, C. F.; Fuller, T. F.; Luzinov, I.; Yushin, G. Toward Efficient Binders for Li-ion Battery Si-based Anodes: Polyacrylic Acid. *ACS Appl. Mater. Interfaces* **2010**, *2*, 3004−3010.

(27) Chen, L.; Xie, X.; Xie, J.; Wang, K.; Yang, J. Binder Effect on Cycling Performance of Silicon/carbon Composite Anodes for Lithium Ion Batteries. *J. Appl. Electrochem.* **2006**, *36*, 1099−1104.

(28) Liu, W.-R.; Yang, M.-H.; Wu, H.-C.; Chiao, S.; Wu, N.-L. Enhanced Cycle Life of Si Anode for Li-ion Batteries by Using Modified Elastomeric Binder. *Electrochem. Solid-State Lett.* **2005**, *8*, A100−A103.

(29) Buqa, H.; Holzapfel, M.; Krumeich, F.; Veit, C.; Novák, P. Study of Styrene Butadiene Rubber and Sodium Methyl Cellulose as Binder for Negative Electrodes in Lithium-ion Batteries. *J. Power Sources* **2006**, *161*, 617−622.

(30) Koo, B.; Kim, H.; Cho, Y.; Lee, K. T.; Choi, N. S.; Cho, J. A Highly Cross-Linked Polymeric Binder for High-Performance Silicon Negative Electrodes in Lithium Ion Batteries. *Angew. Chem., Int. Ed.* **2012**, *51*, 8762−8767.

(31) Han, Z.-J.; Yabuuchi, N.; Hashimoto, S.; Sasaki, T.; Komaba, S. Cross-linked Poly (acrylic acid) with Polycarbodiimide as Advanced Binder for Si/graphite Composite Negative Electrodes in Li-ion Batteries. *ECS Electrochem. Lett.* **2013**, *2*, A17−A20.

(32) Sun, C.; Deng, Y.; Wan, L.; Qin, X.; Chen, G. Graphene Oxide-immobilized NH(2)-terminated Silicon Nanoparticles by Cross-linked Interactions for Highly stable Silicon Negative Electrodes. *ACS Appl. Mater. Interfaces* **2014**, *6*, 11277−11285.

(33) Liu, J.; Zhang, Q.; Wu, Z.-Y.; Wu, J.-H.; Li, J.-T.; Huang, L.; Sun, S.-G. A High-performance Alginate Hydrogel Binder for the Si/C Anode of a Li-ion Battery. *Chem. Commun.* **2014**, *50*, 6386−6389.

(34) Park, Y.; Lee, S.; Kim, S.-H.; Jang, B. Y.; Kim, J. S.; Oh, S. M.; Kim, J.-Y.; Choi, N.-S.; Lee, K. T.; Kim, B.-S. A Photo-cross-linkable Polymeric Binder for Silicon Anodes in Lithium Ion Batteries. *RSC Adv.* **2013**, *3*, 12625−12630.

(35) Kwon, T.-w.; Jeong, Y. K.; Lee, I.; Kim, T. S.; Choi, J. W.; Coskun, A. Systematic Molecular-Level Design of Binders Incorporating Meldrum's Acid for Silicon Anodes in Lithium Rechargeable Batteries. *Adv. Mater.* **2014**, *26*, 7979−7985.

(36) Jeong, Y. K.; Kwon, T.-w.; Lee, I.; Kim, T.-S.; Coskun, A.; Choi, J. W. Hyperbranched β-Cyclodextrin Polymer as an Effective Multidimensional Binder for Silicon Anodes in Lithium Rechargeable Batteries. *Nano Lett.* **2014**, *14*, 864−870.

(37) Yang, S. Y.; Rubner, M. F. Micropatterning of Polymer Thin Films with pH-sensitive and Cross-linkable Hydrogen-bonded Polyelectrolyte Multilayers. *J. Am. Chem. Soc.* **2002**, *124*, 2100−2101.

DOI: 10.1021/acsami.5b06682
ACS Appl. Mater. Interfaces 2015, 7, 23545−23553

(38) Li, Q.; He, R.; Jensen, J. O.; Bjerrum, N. J. Approaches and Recent Development of Polymer Electrolyte Membranes for Fuel Cells Operating above 100 °C. *Chem. Mater.* **2003**, *15*, 4896−4915.
(39) Chuang, S.-W.; Hsu, S. L.-C.; Yang, M.-L. Preparation and Characterization of Fluorine-containing Polybenzimidazole/imidazole Hybrid Membranes for Proton Exchange Membrane Fuel Cells. *Eur. Polym. J.* **2008**, *44*, 2202−2206.
(40) Aurbach, D.; Markovsky, B.; Talyossef, Y.; Salitra, G.; Kim, H.-J.; Choi, S. Studies of Cycling behavior, Ageing, and Interfacial Reactions of $LiNi_{0.5}Mn_{1.5}O_4$ and Carbon Electrodes for Lithium-ion 5-V Cells. *J. Power Sources* **2006**, *162*, 780−789.
(41) Naumov, P.; Jovanovski, G. Infrared Study of the Binuclear Cadmium (II) Imidazole Saccharinato Complex: Comparison with the Copper (II) Compound. *Acta Chim. Slov* **1999**, *46*, 389−404.
(42) Broughton, W.; Mera, R.; Hinopoulos, G. Creep Testing of Adhesive Joints T-Peel Test. *Natl. Phys. Lab. (U.K.), [Rep.] CMMT(A)* **1999**, *193*, 1−16.
(43) Yim, T.; Choi, S. J.; Jo, Y. N.; Kim, T.-H.; Kim, K. J.; Jeong, G.; Kim, Y.-J. Effect of Binder Properties on Electrochemical Performance for Silicon-graphite Anode: Method and Application of Binder Screening. *Electrochim. Acta* **2014**, *136*, 112−120.
(44) Yim, T.; Choi, S. J.; Park, J.-H.; Cho, W.; Jo, Y. N.; Kim, T.-H.; Kim, Y.-J. The Effect of an Elastic Functional Group in a Rigid Binder Framework of Silicon−graphite Composites on Their Electrochemical Performance. *Phys. Chem. Chem. Phys.* **2015**, *17*, 2388−2393.
(45) Yabuuchi, N.; Shimomura, K.; Shimbe, Y.; Ozeki, T.; Son, J. Y.; Oji, H.; Katayama, Y.; Miura, T.; Komaba, S. Graphite-Silicon-Polyacrylate Negative Electrodes in Ionic Liquid Electrolyte for Safer Rechargeable Li-Ion Batteries. *Adv. Energy Mater.* **2011**, *1*, 759−765.
(46) Chan, C. K.; Peng, H.; Liu, G.; McIlwrath, K.; Zhang, X. F.; Huggins, R. A.; Cui, Y. High-performance Lithium Battery Anodes Using Silicon Nanowires. *Nat. Nanotechnol.* **2008**, *3*, 31−35.
(47) Hubaud, A. A.; Yang, Z.; Schroeder, D. J.; Dogan, F.; Trahey, L.; Vaughey, J. T. Interfacial Study of the Role of SiO_2 on Si Anodes Using Electrochemical Quartz Crystal Microbalance. *J. Power Sources* **2015**, *282*, 639−644.

DOI: 10.1021/acsami.5b06682
ACS Appl. Mater. Interfaces 2015, 7, 23545−23553